A&A 562, A33 (2014)
DOI: 10.1051/0004-6361/201322297

Astronomy & Astrophysics

The first submillimeter observation of CO in the stratosphere of Uranus⋆

T. Cavalié[1,2], R. Moreno[3], E. Lellouch[3], P. Hartogh[4], O. Venot[5], G. S. Orton[6], C. Jarchow[4], T. Encrenaz[3], F. Selsis[1,2], F. Hersant[1,2], and L. N. Fletcher[7]

[1] Univ. Bordeaux, LAB, UMR 5804, 33270 Floirac, France
e-mail: cavalie@obs.u-bordeaux1.fr
[2] CNRS, LAB, UMR 5804, 33270 Floirac, France
[3] LESIA – Observatoire de Paris, CNRS, Université Paris 06, Université Paris-Diderot, Meudon, France
[4] Max Planck Institut für Sonnensystemforschung, Katlenburg-Lindau, Germany
[5] Instituut voor Sterrenkunde, Katholieke Universiteit Leuven, Leuven, Belgium
[6] Jet Propulsion Laboratory, California Institute of Technology, Pasadena, USA
[7] Atmospheric, Oceanic and Planetary Physics, Clarendon Laboratory, University of Oxford, Parks Road, Oxford OX1 3PU, UK

Received 17 July 2013 / Accepted 7 November 2013

ABSTRACT

Context. Carbon monoxide (CO) has been detected in all giant planets and its origin is both internal and external in Jupiter and Neptune. Despite its first detection in Uranus a decade ago, the magnitude of its internal and external sources remains unconstrained.
Aims. We targeted CO lines in Uranus in the submillimeter range to constrain its origin.
Methods. We recorded the disk-averaged spectrum of Uranus with very high spectral resolution at the frequencies of CO rotational lines in the submillimeter range in 2011−2012. We used empirical and diffusion models of the atmosphere of Uranus to constrain the origin of CO. We also used a thermochemical model of its troposphere to derive an upper limit on the oxygen-to-hydrogen (O/H) ratio in the deep atmosphere of Uranus.
Results. We have detected the CO(8−7) rotational line for the first time with *Herschel*-HIFI. Both empirical and diffusion models results show that CO has an external origin. An empirical profile in which CO is constant above the 100 mbar level with a mole fraction of $7.1-9.0 \times 10^{-9}$, depending on the adopted stratospheric thermal structure, reproduces the data. Sporadic and steady source models cannot be differentiated with our data. Taking the internal source model upper limit of a mole fraction of 2.1×10^{-9} we find, based on our thermochemical computations, that the deep O/H ratio of Uranus is less than 500 times solar.
Conclusions. Our work shows that the average mole fraction of CO decreases from the stratosphere to the troposphere and thus strongly advocates for an external source of CO in Uranus. Photochemical modeling of oxygen species in the atmosphere of Uranus and more sensitive observations are needed to reveal the nature of the external source.

Key words. planets and satellites: individual: Uranus – planets and satellites: atmospheres – submillimeter: planetary systems

1. Introduction

The detection of water vapor (H_2O) and carbon dioxide (CO_2) in the stratospheres of the giant planets and Titan by Feuchtgruber et al. (1997), Coustenis et al. (1998), Samuelson et al. (1983), and Burgdorf et al. (2006) has raised several questions: what are the sources of oxygen to their upper atmospheres? And do the sources vary from planet to planet? Oxygen-rich deep interiors of the giant planets cannot explain the observations because these species are trapped by condensation below their tropopause (except CO_2 in Jupiter and Saturn). Therefore, several sources in their direct or far environment have been proposed: icy rings and/or satellites (Strobel & Yung 1979), interplanetary dust particles (IDP; Prather et al. 1978), and large comet impacts (Lellouch et al. 1995).

While the relative similarity of the infall fluxes inferred for H_2O by Feuchtgruber et al. (1997) may indicate that IDP could be the source for all giant planets (Landgraf et al. 2002), infrared and far-infrared observations have unveiled a quite different picture. Infrared Space Observatory, *Cassini, Odin*, and *Herschel* observations proove that the Jovian stratospheric H_2O and CO_2 originate from the Shoemaker-Levy 9 (SL9) comet impacts (Lellouch et al. 2002, 2006; Cavalié et al. 2008a, 2012, 2013), while *Herschel* recently shows that the external flux of water at Saturn and Titan is likely due to the Enceladus geysers and the water torus they feed (Hartogh et al. 2011; Moreno et al. 2012).

The situation is even more complex for carbon monoxide (CO). Because CO does not condense at the tropopauses of giant planets, oxygen-rich interiors are also a potential source. An internal component has indeed been observed in the vertical profile of CO in Jupiter by Bézard et al. (2002) and in Neptune, originally by Marten et al. (1993) and Guilloteau et al. (1993), while an upper limit has been set on its magnitude by Cavalié et al. (2009) and Fletcher et al. (2012) for Saturn. The measurement of the tropospheric mole fraction of CO can be used to constrain the deep oxygen-to-hydrogen (O/H) ratio (Lodders & Fegley 1994), which is believed to be representative of condensation processes of the planetesimals that formed the giant planets (Owen et al. 1999; Gautier & Hersant 2005). On the other hand, large comets seem to be the dominant external source, as

⋆ *Herschel* is an ESA space observatory with science instruments provided by European-led Principal Investigator consortia and with important participation from NASA.

Table 1. Summary of the *Herschel*-HIFI observations of CO in Uranus.

Date	OD	Obs. ID	ν [GHz]	Δt [h]	$\theta_{\rm HIFI}$ [″]	$\theta_{\rm Uranus}$ [″]
2011-07-01	779	1342223423	921.800 GHz	1.82	23.0	3.53
2012-06-15	1128	1342247027	921.800 GHz	2.54	23.0	3.47
2012-06-15	1128	1342247028	921.800 GHz	2.54	23.0	3.47
2012-06-15	1128	1342247029	921.800 GHz	2.54	23.0	3.47

Notes. OD means operational day, ν is the CO line center frequency, Δt is the total integration time, $\theta_{\rm HIFI}$ is the *Herschel*-HIFI telescope beamwidth, and $\theta_{\rm Uranus}$ is the equatorial diameter of Uranus.

shown by various studies: Bézard et al. (2002) and Moreno et al. (2003), for Jupiter, Cavalié et al. (2010), for Saturn and Lellouch et al. (2005, 2010), Hesman et al. (2007), Fletcher et al. (2010) and Luszcz-Cook & de Pater (2013), for Neptune.

The first detection of CO in Uranus was obtained by Encrenaz et al. (2004) from fluorescent emission at 4.7 μm. They derived a mixing ratio of 2×10^{-8} by assuming a uniform distribution throughout the atmosphere. The authors tentatively proposed that CO was depleted below the tropopause, suggesting that CO would have an external origin. Despite this first detection almost a decade ago, the situation has remained unclear. Ground-based heterodyne spectroscopy has been used unsuccessfully in the past to try and detect CO in Uranus. Rosenqvist et al. (1992) first set an upper limit of 4×10^{-8} and subsequent attempts to detect CO have failed so far (Marten et al. 1993; Cavalié et al. 2008b). In this paper, we present observations of CO in Uranus carried out with the *Herschel* Space Observatory (Pilbratt et al. 2010) in 2011−2012, which led to the first detection of CO in Uranus in the submillimeter range.

In the following sections, we will describe the observations, their modeling, and our derivations of new constraints on the origin of CO in Uranus and its deep O/H ratio.

2. Observations

We observed the CO(8−7) line at 921.800 GHz with the Heterodyne Instrument for the Far-Infrared (HIFI, de Graauw et al. 2010) aboard *Herschel* (Pilbratt et al. 2010) on July 1, 2011, as part of the guaranteed time key program "Water and related chemistry in the solar system", also known as "*Herschel* solar system Observations" (HssO; Hartogh et al. 2009). The CO(8−7) line was targeted in Uranus for ∼two hours. The resulting spectrum led us to a tentative detection of CO in Uranus at the level of $\sim 2.5\sigma$ (on the line peak) at native resolution and encouraged us to perform a deeper integration of this line.

We obtained an ∼eight-hour integration (split into three observations of equal length) of the same line on June 15, 2012, as part of the *Herschel* open time 2 program OT2_tcavalie_6. We performed the observations in double-beam switch mode with the Wide-Band Spectrometer (WBS) at a nominal spectral resolution of 1.1 MHz (more details given in Table 1). We processed the data with the *Herschel* interactive processing environment (HIPE 9, Ott 2010) up to Level 2 for the horizontal (H) and vertical (V) polarizations and stitched the WBS subbands together. We determined the baseline ripple frequencies caused by the strong continuum emission of Uranus with a normalized periodogram (Lomb 1976) and we removed the three or four strongest sine waves. Those sine waves are caused by the hot and cold black bodies and by the local oscillator chain of the instrument and have periods of 90−100 MHz (Roelfsema et al. 2012). We corrected the double-sideband response of HIFI by assuming a sideband ratio of 1, i.e., a single sideband gain of 0.5

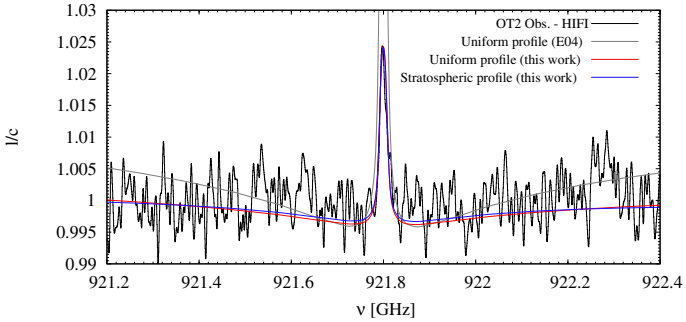

Fig. 1. *Herschel*-HIFI observation of the CO(8−7) line in Uranus on June 15, 2012, expressed in terms of line-to-continuum ratio (l/c, black line). This line can be modeled successfully with either empirical models: (i) a "uniform" profile with a constant mole fraction of 7.2×10^{-9} throughout the atmosphere (red line); and (ii) a "stratospheric" profile with a constant mole fraction of 7.1×10^{-9} above the 100 mbar level and zero below it (blue line). The spectrum resulting from the Encrenaz et al. (2004) uniform source profile is also shown for comparison (grey line, labeled "E04"). The synthetic lines are obtained with the thermal profile of Feuchtgruber et al. (2013).

(Roelfsema et al. 2012), and identical continuum levels in both sidebands. The uncertainty on the sideband ratio is 12% (3% on the single sideband gain), and the continuum levels in the two sidebands should differ by less than 1%, according to our model. Finally, we coadded the H and V polarizations after weighting them according to their respective noise levels (the V spectra were always noisier than the H spectra). We obtained a clear detection at the level of 7σ on the line peak, at a smoothed resolution of 8 MHz using a gaussian lineshape, on the combined eight-hour observation shown in Fig. 1. Because we have not performed any absolute calibration, we analyze this line in terms of line-to-continuum ratio (l/c). The observed continuum levels differ by 6% in the H and V polarizations, and so we have to account for an additional uncertainty of 3% on the continuum level of our averaged spectrum.

We note that we also targeted the CO (3−2) and (6−5) lines (at 345.796 GHz and 691.473 GHz, respectively) in Uranus using the Heterodyne Receiver Array Programme (HARP) receiver array and the D-band receiver, respectively, of the *James Clerk Maxwell* Telescope (JCMT) on October 15−16 and November 2, 2009, as part of the M09BI02 project. These observations resulted in the determination of an upper limit of 6×10^{-8} uniform with altitude up to the CO homopause for the CO mole fraction and will not be discussed further.

3. Models and results

3.1. Radiative transfer model

We performed all spectral line computations with the forward radiative transfer model detailed in Cavalié et al. (2008b, 2013),

adapted to Uranus. This line-by-line model accounts for the elliptical geometry of the planet and its rapid rotation. Opacity due to H_2-He-CH_4 collision-induced absorption (Borysow et al. 1985, 1988; Borysow & Frommhold 1986) was included. Orton et al. (2007) published H_2-H_2 collision-induced coefficient tables, which reproduce the continuum of Uranus between 700 and 1100 cm^{-1} as observed by *Spitzer* better, but these coefficients do not differ significantly in the wavelength range of our observations. We used the JPL Molecular Spectroscopy catalog Pickett et al. (1998) and the H_2/He pressure-broadening parameters for CO lines from Sung & Varanasi (2004) and Mantz et al. (2005), i.e., a collisional linewidth at 300 K of 0.0661 cm^{-1} atm^{-1} for the CO(8−7) line and a temperature dependence exponent of 0.638. We used the thermal profiles of Feuchtgruber et al. (2013) and Orton et al. (2013a). They have the same tropopause temperature (53 K), but the profile of Feuchtgruber et al. (2013) is continuously warmer than the profile of Orton et al. (2013a) in the stratosphere (by 2 K at 10 mbar, 5 K at 1 mbar, and 11 K at 0.1 mbar). We present results for both thermal profiles hereafter. We smoothed all synthetic lines to the working resolution of 8 MHz using a gaussian lineshape.

The CO line is optically thin with $\tau = 0.04-0.25$ (depending on models) and probes the stratosphere of Uranus between the 0.1 and 5 mbar levels, allowing us to derive information on the CO abundance. The signal-to-noise ratio (S/N) of the observations results in error bars of 14%. By adding this uncertainty quadratically with other uncertainty sources (sideband ratio, continuum levels), we end up with an uncertainty of 19% on the results presented hereafter.

3.2. Empirical models

We tested two classes of empirical models: (i) uniform profiles (referred to as "uniform" hereafter); and (ii) uniform profiles in the stratosphere down to a cutoff pressure level (referred to as "stratospheric" hereafter). These profiles are not physically plausible mainly due to the low homopause in Uranus (see next subsection), but were considered for comparison with Encrenaz et al. (2004) and Teanby & Irwin (2013). Our results are described hereafter and are summarized in Table 2.

The uniform distribution of Encrenaz et al. (2004) with a CO mole fraction of 2×10^{-8} overestimates the observed line core by a factor of 2.5−3. The observed line can be fitted with a "uniform" profile in which the CO mole fraction is 7.2×10^{-9} with the profile of Feuchtgruber et al. (2013), or 9.3×10^{-9} with the profile of Orton et al. (2013a).

The line can be fitted equally well with a "stratospheric" profile in which the CO is constant above the 100 mbar level with a CO mole fraction of 7.1×10^{-9} with the thermal profile of Feuchtgruber et al. (2013), or 9.0×10^{-9} with the profile of Orton et al. (2013a). For comparison with other papers (e.g., Encrenaz et al. 2004; Cavalié et al. 2008b; Teanby & Irwin 2013), we set this transition level to 100 mbar, but our computations show this level could be located anywhere between ∼3 and 1000 mbar. Our results in terms of mole fraction would be affected by less than 10%. If set above the 3 mbar level, then more CO would be needed.

From these empirical models, it is not possible to favor an internal or an external origin for CO in the atmosphere of Uranus because the models cannot be distinguished (see Fig. 1).

Fortunately, Teanby & Irwin (2013) recently published *Herschel*-SPIRE observations at CO line wavelengths. These observations are sensitive to the 10−2000 mbar range, with a contribution function peak at 200 mbar (see their Fig. 2b), and they did not result in any detection. Those authors have set a stringent upper limit of 2.1×10^{-9} on the CO mole fraction in their internal source model. This is ∼3−5 times lower than required by our observations. It is thus a clear indication that the HIFI line is caused by external CO.

Table 2. Summary of the empirical and diffusion model results.

Empirical model		
Thermal profile	Uniform	Stratospheric
Feuchtgruber	7.2×10^{-9}	7.1×10^{-9}
Orton	9.3×10^{-9}	9.0×10^{-9}

Diffusion model			
Thermal profile	Internal source	External source	
	y_{CO}	ϕ_{CO}	y_0
Feuchtgruber	1.9×10^{-8}	2.2×10^{5}	3.1×10^{-7}
Orton	2.7×10^{-8}	2.7×10^{5}	3.9×10^{-7}

Notes. All results are mole fractions, except ϕ_{CO} (in cm^{-2} s^{-1}). The cutoff level in the "stratospheric" empirical model is at 100 mbar. The internal source value of y_{CO} in the diffusion model enables fitting the CO line core amplitude, but the line is too broad and additional broad wings incompatible with the data are generated.

3.3. Diffusion model

Uranus has the lowest homopause amongst the giant planets (Orton et al. 1987; Moses et al. 2005). It is located around the 1 mbar level, where submillimeter observations generally probe. Therefore, we computed more realistic CO vertical profiles by accounting for diffusion processes to see how our previous results are impacted by the low homopause of Uranus. Such modeling also shows how the various external sources can be parametrized.

The vertical profile of CO primarily depends on the sources of CO, but it is also influenced by other oxygen sources. Indeed, O produced by H_2O photolysis reacts with CH_3 and other hydrocarbons to produce CO (Moses et al. 2000). The magnitude of the H_2O flux is still quite uncertain, mostly due to limitations in the knowledge of the thermal structure and eddy mixing at the time of the observations of Feuchtgruber et al. (1997). For the sake of simplicity, we ignored (photo-)chemical processes.

We adapted the 1D time-dependent model of Dobrijevic et al. (2010, 2011) to Uranus and removed all photochemical processes. Orton et al. (2013b) constrained the stratospheric K_{zz} within [1000:1500] cm^2 s^{-1} (vertically constant) with CH_4 and C_2H_6 *Spitzer* observations. We took their best fit value (1200 cm^2 s^{-1}) in our model. We tested three sources of CO, representing simple cases: (i) an internal source; (ii) a steady flux of micrometeorites (IDP); and (iii) a single large comet impact[1]. The three sources tested are controlled by a few parameters: (i) the tropospheric CO mole fraction y_{CO} for an internal source; (ii) the flux ϕ_{CO} at the upper boundary of the model atmosphere for a steady source; and (iii) the equivalent mole fraction of CO y_0 deposited by a comet and averaged over the planet. We assumed that all the CO was deposited at levels higher than 0.1 mbar in analogy to the SL9 impacts (Lellouch et al. 1995; Moreno et al. 2003) and that the impact time $\Delta t \sim 300$ years as it roughly corresponds to the diffusion

[1] This does not exclude a combination of internal and external sources, or any intermediate situation between a continuum of micrometeoritic impacts and a single impact event.

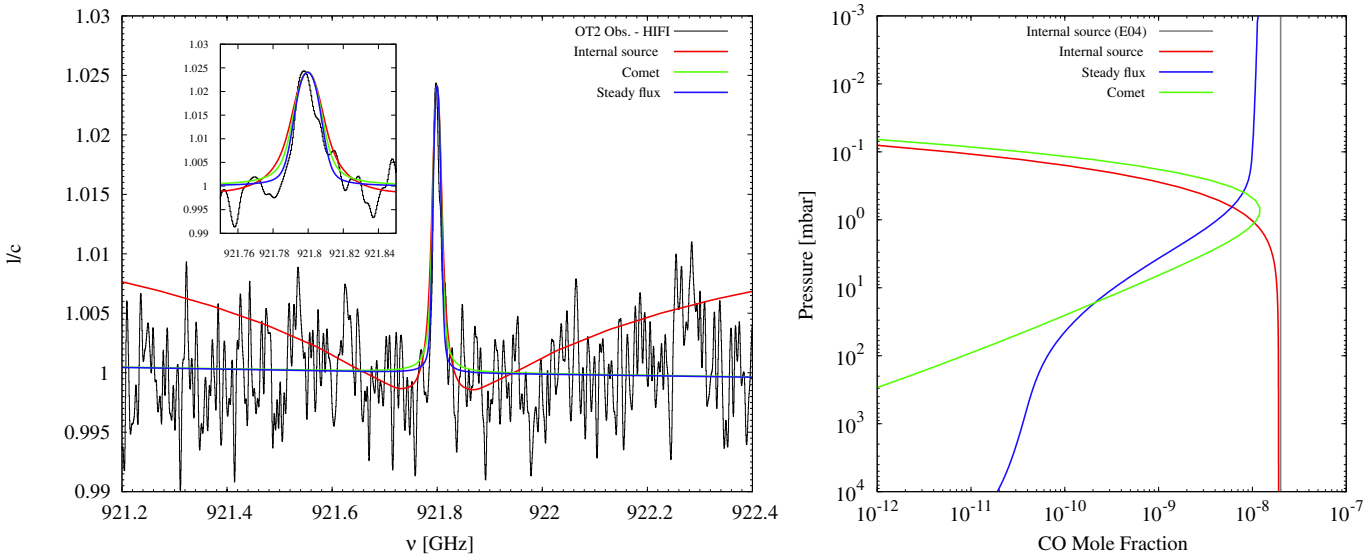

Fig. 2. *Left*: *Herschel*-HIFI observation of the CO(8−7) line in Uranus on June 15, 2012, expressed in terms of line-to-continuum ratio (l/c, black line). For each source, the models that best fit the emission core are displayed: an internal source yielding a mole fraction of 1.9×10^{-8} in the upper troposphere (red line), a steady external flux (due to IDP or a local source) of 2.2×10^5 cm^{-2} s^{-1} (blue line), and a comet with a diameter of 640 m depositing 3.4×10^{13} g of CO above the 0.1 mbar level ∼300 years ago (green line). These models were computed with the thermal profile of Feuchtgruber et al. (2013). The internal source model overestimates the line core width and produces a broad absorption that is not observed in the data. The external source models can barely be differentiated. *Right*: vertical profiles associated with the spectra.

time down to 1 mbar in Uranus in our model, but other combinations of deposition time and level are possible. To infer the mass and diameter of the comet, we assumed the comet density was 0.5 g cm^{-3} (Weissman et al. 2004; Davidsson et al. 2007) and that the comet yielded 50% CO at impact (Lellouch et al. 1997).

The vertical profiles and resulting spectra corresponding to the three sources, as obtained with the thermal profile of Feuchtgruber et al. (2013), are displayed in Fig. 2. The best fits to the spectrum are obtained for external source models. Despite resulting in different vertical profiles, a steady flux $\phi_{CO} = 2.2 \times 10^5$ cm^{-2} s^{-1} and a 640 m diameter comet depositing 3.5×10^{13} g of CO ($y_0 = 3.1 \times 10^{-7}$) result in lines that are indistinguishable from the standpoint of our observations. Such impact at Uranus occurs every ∼500 years with a factor of 6 uncertainty (Zahnle et al. 2003). Such timescales are fully compatible with our assumption on Δt. With the thermal profile of Orton et al. (2013a), we obtain slightly higher values because of lower stratospheric temperatures: $\phi_{CO} = 2.7 \times 10^5$ cm^{-2} s^{-1} and $y_0 = 3.9 \times 10^{-7}$ (i.e., a 700 m diameter comet). All fit parameters are listed in Table 2. These values remain to be confirmed by more rigorous (photochemical) modeling and higher S/N data.

The amplitude of the CO emission peak is reproduced with an internal source model in which $y_{CO} = 1.9 \times 10^{-8}$ (see Fig. 2). With the thermal profile of Orton et al. (2013a), $y_{CO} = 2.7 \times 10^{-8}$. We note that ∼three times more tropospheric CO is needed in this model, compared to the "uniform" empirical model value derived in Sect. 3.2. This is due to the fact that the observed emission line probes the mbar level, i.e., where the CO vertical profile sharply decreases because of the low homopause in the atmosphere of Uranus. As a result, a stronger internal source is required to reach a sufficient level of abundance of CO around the mbar level. The main outcome of this model is that it now overestimates the line core width and results in additional broad absorption because CO is much more abundant in the lower stratosphere than in the external source models (by as much as two orders of magnitude at 10 mbar). The absence of such a broad CO absorption in the data cannot be caused by our sinusoidal ripple removal procedure because we have removed sine waves of much shorter period than the total width of such broad absorption wings. We can rule out the internal source model because the width of the line core is not fitted, there is no broad absorption in the spectrum, and the derived y_{CO} values are an order of magnitude larger than the upper limit set by *Herschel*-SPIRE observations of this region of the atmosphere (Teanby & Irwin 2013). Thus, as long as there is no significant photochemical source of CO in the stratosphere, the HIFI line is caused by external CO.

3.4. An upper limit on the deep O/H ratio in Uranus

Thermochemistry in the deep interior of Uranus links the CO abundance to H_2O abundance and thus to the internal O/H ratio (Fegley & Prinn 1988; Lodders & Fegley 1994) with the following net thermochemical equilibrium reaction,

$$H_2O + CH_4 = CO + 3H_2.$$

The upper tropospheric mole fraction of CO is fixed at the level where the thermochemical equilibrium is quenched by vertical diffusion.

The upper limit of Teanby & Irwin (2013) on the internal source ($y_{CO} = 2.1 \times 10^{-9}$) can be further used to try and constrain the deep atmospheric O/H ratio in Uranus. Their observations probe between 10 and 2000 mbar, i.e., well below the homopause level (see Fig. 2 right). As a consequence, this upper limit is valid even if the authors have not accounted for the low homopause of Uranus.

We have adapted the thermochemical model developed by Venot et al. (2012) to Uranus to constrain the O/H ratio. This model accounts for C, N, and O species. We extended our thermal profile to high pressures following the dry adiabat. The profiles of Feuchtgruber et al. (2013) and Orton et al. (2013a) are similar in the upper troposphere and thus give similar deep tropospheric profiles. We constrained the O/H and C/H ratios by fitting the following upper tropospheric mole fractions with errors

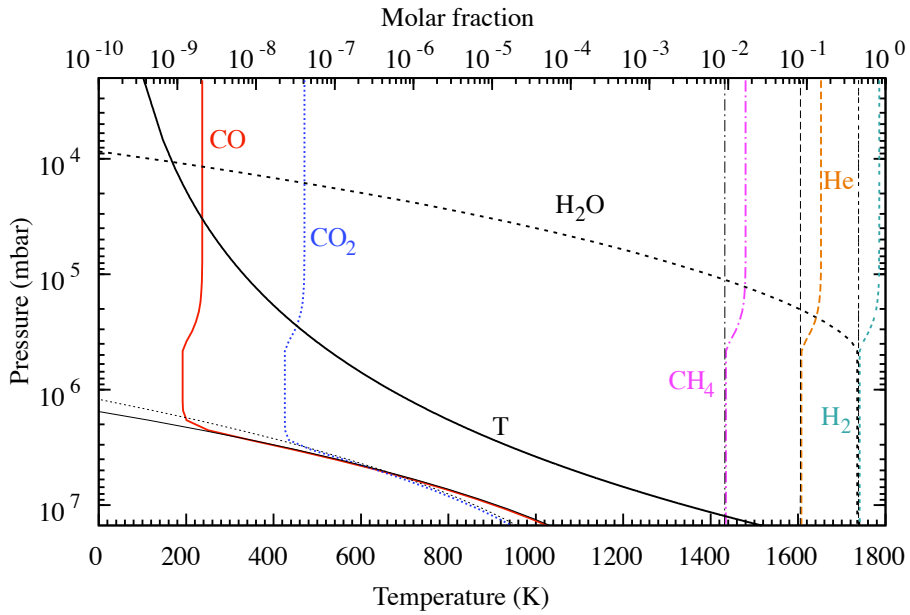

Fig. 3. Molar fraction profiles in the troposphere of Uranus obtained with the model of Venot et al. (2012), targeting the 2.1×10^{-9} upper limit on the upper tropospheric CO mole fraction obtained by Teanby & Irwin (2013). The temperature profile in the troposphere is shown with a solid black line. Thermochemical equilibrium profiles are plotted in black with the same layout as their corresponding species. CO and CO_2 are quenched around $2-3 \times 10^6$ mbar. H_2O departs from thermochemical equilibrium because of condensation and causes an increase of other species mole fractions (the sum of all mole fractions is normalized to unity at all levels). The model parameters are: O/H = 501⊙, C/H = 18⊙, and $K_{zz} = 10^8$ cm^2 s^{-1}.

lower than 4%: 0.152 for He (Conrath et al. 1987), 0.016 for CH_4 (Baines et al. 1995; Sromovsky & Fry 2008), and the 2.1×10^{-9} upper limit for CO. The level at which CO is quenched depends not only on the temperature profile and the deep O/H ratio, but also on the deep K_{zz}. By assuming Uranus' interior is convective, we estimate K_{zz} from the planet's internal heat flux (Stone 1976). Following Pearl et al. (1990), $K_{zz} \sim 10^8$ cm^2 s^{-1}, within one order of magnitude (Lodders & Fegley 1994). The resulting tropospheric vertical profiles for this nominal model are shown in Fig. 3. The elemental ratios in this model are 501 times solar for O/H and 18 times solar for C/H (with solar abundances, ⊙ hereafter, taken from Asplund et al. 2009). The N species have no significant impact on the C and O species. We also computed the elemental ratios in a series of additional models to evaluate the influence of parameters like K_{zz} and the upper tropospheric CH_4 mole fraction on the O/H ratio. The results are displayed in Table 3. We find that the deep O/H is lower than ∼500⊙ (nominal model), but could be even below 340⊙ to be in agreement with the CO tropospheric upper limit in all cases. On Neptune, Luszcz-Cook & de Pater (2013) find that "an upwelled CO mole fraction of 0.1 ppm implies a global O/H enrichment of at least 400, and likely more than 650 times the protosolar value".

Table 3. Summary of the thermochemical model results.

Model	K_{zz} cm^2 s^{-1}	y_{CH_4} $\times 10^{-2}$	C/H $\times$⊙^{a}	y_{CO} $\times 10^{-9}$	O/H $\times$⊙^{b}
Nominal	10^8	1.6^c	18	2.1	501
CH_4-rich	10^8	3.2^d	40	2.1	417
low K_{zz}	10^7	1.6	13	2.1	631
high K_{zz}	10^9	1.6	23	2.1	339

Notes. We obtained values so as to reach the 2.1×10^{-9} upper limit of Teanby & Irwin (2013) for the CO upper tropospheric mole fraction. [(a)] Solar C/H volume ratio: 2.69×10^{-4} (Asplund et al. 2009). [(b)] Solar O/H volume ratio: 4.90×10^{-4} (Asplund et al. 2009). [(c)] Baines et al. (1995) and Sromovsky & Fry (2008). [(d)] Fry et al. (2013); Sromovsky et al. (2011); and Karkoschka & Tomasko (2009).

4. Discussion and conclusion

We detected the CO(8−7) line at 921.800 GHz in Uranus with *Herschel* and we constrained its possible sources.

Herschel-HIFI (this work) and *Herschel*-SPIRE (Teanby & Irwin 2013) results show that the average CO mole fraction is decreasing from the stratosphere to the troposphere. This suggests the deep interior is not the source of the observed CO. Our diffusion model calculations confirm that the internal source hypothesis is not valid and show that Uranus has an external source of CO as long as there is not a significant photochemical source of CO in the stratosphere. The data can be successfully fitted with an empirical model in which CO has a mole fraction of $7.1-9.0 \times 10^{-9}$ above the 100 mbar level (value depending on the chosen thermal profile). There is a contradiction between this model's mole fraction values and the mole fraction reported by Encrenaz et al. (2004) (3×10^{-8} in their external source model). Regarding this apparent discrepancy, we note that modeling LTE emission from CO rotational lines is much simpler than inferring an abundance from non-LTE fluorescence (e.g., López-Valverde et al. 2005). At any rate, a reanalysis of the Encrenaz et al. (2004) data in the light of CO distributions proposed in this paper should be performed.

Comet and steady source models, in which diffusion processes are accounted for, give very similar fit to the data. These results should be confirmed with more elaborate models, i.e., photochemical models and more sensitive observations. Oxygen photochemistry computations, taking nearly concomitant measurements of the thermal profile (Feuchtgruber et al. 2013; Orton et al. 2013a), of the influx of H_2O (Jarchow et al., in prep.), and

of the influx of CO_2 (Orton et al. 2013b), into account would enable us to draw better constraints on the external source of oxygen. It would certainly reduce the external flux of CO or the mass of the impacting comet we obtained from a simple diffusion model because the chemical conversion of H_2O into CO would already provide a significant part of the observed stratospheric column of CO.

We used the internal source upper limit derived by Teanby & Irwin (2013) ($y_{CO} = 2.1 \times 10^{-9}$), which also contradicts the detection level of Encrenaz et al. (2004) (2×10^{-8} in their internal source model), to derive an upper limit on the deep O/H ratio of Uranus. Our thermochemical simulations show that the deep O/H ratio is lower than 500⊙, which provides a y_{CO} value lower than 2.1×10^{-9}. A dedicated probe, as in the mission concepts proposed by Arridge et al. (2014) and Mousis et al. (2014) in response to the ESA 2013 Call for White Papers for the Definition of the L2 and L3 Missions in the ESA Science Programme, or radio observations might be the only way to measure the deep O/H ratio in Uranus.

Acknowledgements. T. Cavalié acknowledges funding from the Centre National d'Études Spatiales (CNES). T. Cavalié and F. Selsis acknowledge support from the European Research Council (Starting Grant 209622: E_3ARTHs). O. Venot acknowledges support from the KU Leuven IDO project IDO/10/2013 and from the FWO Post-doctoral Fellowship programme. G. Orton acknowledges funding from the National Aeronautics and Space Administration to the Jet Propulsion Laboratory, California Institute of Technology. L. N. Fletcher was supported by a Royal Society Research Fellowship at the University of Oxford. The authors thank M. Hofstadter for his constructive review. HIFI has been designed and built by a consortium of institutes and university departments from across Europe, Canada, and the United States under the leadership of SRON Netherlands Institute for Space Research, Groningen, The Netherlands, and with major contributions from Germany, France, and the US. Consortium members are: Canada: CSA, U.Waterloo; France: CESR, LAB, LERMA, IRAM; Germany: KOSMA, MPIfR, MPS; Ireland, NUI Maynooth; Italy: ASI, IFSI-INAF, Osservatorio Astrofisico di Arcetri-INAF; Netherlands: SRON, TUD; Poland: CAMK, CBK; Spain: Observatorio Astronómico Nacional (IGN), Centro de Astrobiología (CSIC-INTA). Sweden: Chalmers University of Technology – MC2, RSS & GARD; Onsala Space Observatory; Swedish National Space Board, Stockholm University – Stockholm Observatory; Switzerland: ETH Zurich, FHNW; USA: Caltech, JPL, NHSC. The *James Clerk Maxwell* Telescope is operated by the Joint Astronomy Centre on behalf of the Science and Technology Facilities Council of the UK, the National Research Council of Canada, and the Netherlands Organisation for Scientific Research.

References

Arridge, C., Agnor, C., Ambrosi, R. M., et al. 2014, Planet. Space Sci., submitted
Asplund, M., Grevesse, N., Sauval, A. J., & Scott, P. 2009, ARA&A, 47, 481
Baines, K. H., Mickelson, M. E., Larson, L. E., & Ferguson, D. W. 1995, Icarus, 114, 328
Bézard, B., Lellouch, E., Strobel, D., Maillard, J.-P., & Drossart, P. 2002, Icarus, 159, 95
Borysow, A., & Frommhold, L. 1986, ApJ, 304, 849
Borysow, J., Trafton, L., Frommhold, L., & Birnbaum, G. 1985, ApJ, 296, 644
Borysow, J., Frommhold, L., & Birnbaum, G. 1988, ApJ, 326, 509
Burgdorf, M., Orton, G., van Cleve, J., Meadows, V., & Houck, J. 2006, Icarus, 184, 634
Cavalié, T., Billebaud, F., Biver, N., et al. 2008a, Planet. Space Sci., 56, 1573
Cavalié, T., Billebaud, F., Fouchet, T., et al. 2008b, A&A, 484, 555
Cavalié, T., Billebaud, F., Dobrijevic, M., et al. 2009, Icarus, 203, 531
Cavalié, T., Hartogh, P., Billebaud, F., et al. 2010, A&A, 510, A88
Cavalié, T., Biver, N., Hartogh, P., et al. 2012, Planet. Space Sci., 61, 3
Cavalié, T., Feuchtgruber, H., Lellouch, E., et al. 2013, A&A, 553, A21
Conrath, B., Hanel, R., Gautier, D., Marten, A., & Lindal, G. 1987, J. Geophys. Res., 92, 15003
Coustenis, A., Salama, A., Lellouch, E., et al. 1998, A&A, 336, L85
Davidsson, B. J. R., Gutiérrez, P. J., & Rickman, H. 2007, Icarus, 187, 306
de Graauw, T., Helmich, F. P., Phillips, T. G., et al. 2010, A&A, 518, L6
Dobrijevic, M., Cavalié, T., Hébrard, E., et al. 2010, Planet. Space Sci., 58, 1555
Dobrijevic, M., Cavalié, T., & Billebaud, F. 2011, Icarus, 214, 275
Encrenaz, T., Lellouch, E., Drossart, P., et al. 2004, A&A, 413, L5
Fegley, B., & Prinn, R. G. 1988, ApJ, 324, 621
Feuchtgruber, H., Lellouch, E., de Graauw, T., et al. 1997, Nature, 389, 159
Feuchtgruber, H., Lellouch, E., Orton, G., et al. 2013, A&A, 551, A126
Fletcher, L. N., Drossart, P., Burgdorf, M., Orton, G. S., & Encrenaz, T. 2010, A&A, 514, A17
Fletcher, L. N., Swinyard, B., Salji, C., et al. 2012, A&A, 539, A44
Fry, P. M., Sromovsky, L. A., Karkoschka, E., et al. 2013, in AAS/Division for Planetary Sciences Meeting Abstracts, 45, #312.18
Gautier, D., & Hersant, F. 2005, Space Sci. Rev., 116, 25
Guilloteau, S., Dutrey, A., Marten, A., & Gautier, D. 1993, A&A, 279, 661
Hartogh, P., Lellouch, E., Crovisier, J., et al. 2009, Planet. Space Sci., 57, 1596
Hartogh, P., Lellouch, E., Moreno, R., et al. 2011, A&A, 532, L2
Hesman, B. E., Davis, G. R., Matthews, H. E., & Orton, G. S. 2007, Icarus, 186, 342
Karkoschka, E., & Tomasko, M. 2009, Icarus, 202, 287
Landgraf, M., Liou, J.-C., Zook, H. A., & Grün, E. 2002, AJ, 123, 2857
Lellouch, E., Paubert, G., Moreno, R., et al. 1995, Nature, 373, 592
Lellouch, E., Bézard, B., Moreno, R., et al. 1997, Planet. Space Sci., 45, 1203
Lellouch, E., Bézard, B., Moses, J. I., et al. 2002, Icarus, 159, 112
Lellouch, E., Moreno, R., & Paubert, G. 2005, A&A, 430, L37
Lellouch, E., Bézard, B., Strobel, D. F., et al. 2006, Icarus, 184, 478
Lellouch, E., Hartogh, P., Feuchtgruber, H., et al. 2010, A&A, 518, L152
Lodders, K., & Fegley, Jr., B. 1994, Icarus, 112, 368
Lomb, N. R. 1976, Ap&SS, 39, 447
López-Valverde, M. A., Lellouch, E., & Coustenis, A. 2005, Icarus, 175, 503
Luszcz-Cook, S. H., & de Pater, I. 2013, Icarus, 222, 379
Mantz, A. W., Malathy Devi, V., Chris Benner, D., et al. 2005, J. Mol. Struct., 742, 99
Marten, A., Gautier, D., Owen, T., et al. 1993, ApJ, 406, 285
Moreno, R., Marten, A., Matthews, H. E., & Biraud, Y. 2003, Planet. Space Sci., 51, 591
Moreno, R., Lellouch, E., Lara, L. M., et al. 2012, Icarus, 221, 753
Moses, J. I., Lellouch, E., Bézard, B., et al. 2000, Icarus, 145, 166
Moses, J. I., Fouchet, T., Bézard, B., et al. 2005, J. Geophys. Res., 110, 8001
Mousis, O., Fletcher, L. N., Lebreton, J.-P., et al. 2014, Planet. Space Sci., submitted
Orton, G. S., Aitken, D. K., Smith, C., et al. 1987, Icarus, 70, 1
Orton, G. S., Gustafsson, M., Burgdorf, M., & Meadows, V. 2007, Icarus, 189, 544
Orton, G. S., Fletcher, L. N., Moses, J. I., et al. 2013a, Icarus, submitted
Orton, G. S., Moses, J. I., Fletcher, L. N., et al. 2013b, Icarus, submitted
Ott, S. 2010, in Astronomical Data Analysis Software and Systems XIX, eds. Y. Mizumoto, K.-I. Morita, & M. Ohishi, PASP, 434, 139
Owen, T., Mahaffy, P., Niemann, H. B., et al. 1999, Nature, 402, 269
Pearl, J. C., Conrath, B. J., Hanel, R. A., & Pirraglia, J. A. 1990, Icarus, 84, 12
Pickett, H. M., Poynter, I. R. L., Cohen, E. A., et al. 1998, J. Quant. Spectr. Rad. Transf., 60, 883
Pilbratt, G. L., Riedinger, J. R., Passvogel, T., et al. 2010, A&A, 518, L1
Prather, M. J., Logan, J. A., & McElroy, M. B. 1978, ApJ, 223, 1072
Roelfsema, P. R., Helmich, F. P., Teyssier, D., et al. 2012, A&A, 537, A17
Rosenqvist, J., Lellouch, E., Romani, P. N., Paubert, G., & Encrenaz, T. 1992, ApJ, 392, L99
Samuelson, R. E., Maguire, W. C., Hanel, R. A., et al. 1983, J. Geophys. Res., 88, 8709
Sromovsky, L. A., & Fry, P. M. 2008, Icarus, 193, 252
Sromovsky, L. A., Fry, P. M., & Kim, J. H. 2011, Icarus, 215, 292
Stone, P. H. 1976, in Proc. Colloq. Jupiter: Studies of the Interior, Atmosphere, Magnetosphere and Satellites, ed. T. Gehrels (Univ. of Arizona Press), 586
Strobel, D. F., & Yung, Y. L. 1979, Icarus, 37, 256
Sung, K., & Varanasi, P. 2004, J. Quant. Spectr. Rad. Transf., 85, 165
Teanby, N. A., & Irwin, P. G. J. 2013, ApJ, 775, L49
Venot, O., Hébrard, E., Agúndez, M., et al. 2012, A&A, 546, A43
Weissman, P. R., Asphaug, E., & Lowry, S. C. 2004, in Comets II, eds. M. C. Festou, H. U. Keller, & H. A. Weaver (Univ. of Arizona Press), 337
Zahnle, K., Schenk, P., Levison, H., & Dones, L. 2003, Icarus, 163, 263